

Reactions of NO⁺ with Isomeric Butenes from 225 to 500 K[†]

Anthony J. Midey, Skip Williams, and A. A. Viggiano*

Air Force Research Laboratory, Space Vehicles Directorate,
Hanscom Air Force Base, Massachusetts 01731-3010

Received: May 23, 2000; In Final Form: October 24, 2000

The rate constants and branching fractions have been measured for the reaction of NO⁺ with the four butene isomers of C₄H₈ from 225 to 500 K in a variable temperature-selected ion flow tube. The *cis*- and *trans*-2-butene isomers react at the collision rate via charge transfer over the entire temperature range. Isobutene also reacts at the collision rate at all temperatures, primarily through charge transfer; however, an association channel also competes effectively at the lowest temperatures studied because the charge transfer reaction is only 0.02 eV exothermic. The reaction of NO⁺ with 1-butene is much slower than observed for the other butenes and has a negative temperature dependence. The negative temperature dependence is consistent with the predominant product channel being association. Other products are also observed with 1-butene, including C₄H₇⁺ from hydride transfer, C₄H₈⁺ from charge transfer at higher temperatures, and several other products involving significant rearrangement and chemical bond formation.

Introduction

It is well-known that combustion environments maintain high ionization levels that are typically in the 10⁹–10¹² cm⁻³ range at atmospheric pressure. In most cases, the initial ionization step is attributed primarily to the chemiionization reaction CH + O → HCO⁺ + e⁻. The reactions that follow are numerous and have been the topic of many experimental and theoretical studies. Two areas of recent interest involving the effects of ionization in combustion pertain to particulate formation and combustion enhancement in hydrocarbon fuels. Particulate formation via ionization was first proposed by Calcote and co-workers and involves the formation of large (>C₁₀) polyaromatic hydrocarbon ions which serve as nucleation sites for complex molecular growth processes.^{1–3} Renewed interest in the development of high-speed air-breathing propulsion technology⁴ has prompted a number of investigators to consider adopting plasmas as ignition and piloting aids in supersonic combustors with positive results.^{5–7} Combustion enhancement is currently being studied in this laboratory, focusing on ignition and flame propagation enhancement via ionic pathways.

Computational studies attempting to assess the importance of ionic mechanisms such as those described above have been impeded by a lack of kinetic data at relevant combustion temperatures.⁸ However, the database of ion–molecule chemistry available for the combustion models has expanded substantially in the past few years.^{9–17} The rate constants and branching ratios for the reactions of air plasma ions with numerous alkanes^{9–12} and aromatics^{13–17} have already been studied as a function of temperature in a variable temperature-selected ion flow tube (VT-SIFT) up to 500 K. These measurements have been extended to temperatures greater than 1000 K for benzene,¹⁴ naphthalene,¹⁶ and several alkylbenzenes¹⁷ using a high-temperature flowing afterglow.

Automotive, diesel, aviation, and rocket fuels are mixtures of a large number of hydrocarbons that meet general physical

property specifications. These properties include volatility, freeze point, and heat of combustion to name a few. These operational specifications determine the relative portion of the various classes of species including alkanes, alkenes, and aromatics. The current experiments further expand the series of reactions studied to include alkenes, in this case, the four isomers of butene (C₄H₈). The isomeric butenes have not been studied as extensively as many other hydrocarbon systems, presumably because of their complexity. Furthermore, few quantitative reports of the rates of reaction are available and no temperature-dependent studies have been done. In this paper, the rate constants and branching fractions measured in the VT-SIFT from 225 to 500 K for the reactions of NO⁺ with 1-butene, *cis*-2-butene, *trans*-2-butene, and isobutene (2-methylpropene) are reported. The current results are discussed in light of some previous work.^{13,18}

Experimental Section

The variable temperature-selected ion flow tube (VT-SIFT) has been described in detail elsewhere.¹⁹ Therefore, only details pertaining to the present experiment are described here. The primary NO⁺ ions are generated in a high-pressure ion source by electron impact on NO and are mass selected by a quadrupole mass spectrometer. The selected ions are injected into a fast flow of helium buffer gas. Nitrogen gas is introduced at an inlet upstream from the first reactant inlet to quench electronically and vibrationally excited NO⁺ ions injected into the flow tube. NO⁺ (A) charge transfers to N₂ so that the N₂⁺ signal provides a way to quantify the amount of NO⁺ produced.²⁰ The source conditions used generate ≤2% of the electronically excited NO⁺ which is monitored via charge transfer to N₂.²⁰

A series of cooling lines and heating elements allow the flow tube temperature to be varied from 80 to 500 K. However, the freezing points of the reactants studied here restrict the lowest temperature studied to 225 K. The NO⁺ reactant ions thermally equilibrate in the region upstream from the reactant inlets. Any remaining reactant ions and all of the product ions are sampled downstream through a small orifice and mass analyzed in a

[†] Part of the special issue "Harold Johnston Festschrift".

* To whom correspondence should be addressed. E-mail: albert.viggiano@hanscom.af.mil.

TABLE 1: Rate Constants and Branching Fractions for the Reaction of NO⁺ with the Four Isomers of butene (C₄H₈) from 225 to 500 K Measured in the Variable Temperature-Selected Ion Flow Tube^a

reaction (neutral IP)	products	product ion mass (amu)	$\Delta H_{\text{rxn}}^{298}$	rate constant ($10^{-9} \text{ cm}^3 \text{ s}^{-1}$) [k_c] branching fractions			
				225 K	298 K	400 K	500 K
NO ⁺ + <i>cis</i> -2-C ₄ H ₈ → (9.11 eV)	<i>cis</i> -2-C ₄ H ₈ ⁺ + NO	56	-0.15	1.7 [1.6] >0.99	1.4 [1.6] 1.00	1.6 [1.6] 1.00	1.6 [1.6] 1.00
NO ⁺ + <i>trans</i> -2-C ₄ H ₈ → (9.11 eV)	<i>trans</i> -2-C ₄ H ₈ ⁺ + NO	56	-0.15	1.6 [1.6] >0.99	1.4 [1.5] 1.00	1.7 [1.5] 1.00	1.6 [1.5] 1.00
NO ⁺ + <i>iso</i> -C ₄ H ₈ → (9.24 eV)	<i>iso</i> -C ₄ H ₈ NO ⁺ <i>iso</i> -C ₄ H ₈ ⁺ + NO	86 56	-0.02	1.8 [1.7] 0.33 0.67	1.5 [1.7] 0.15 0.85	1.7 [1.6] 0.03 0.97	1.7 [1.6] 1.00
NO ⁺ + 1-C ₄ H ₈ → (9.58 eV)	C ₄ H ₈ NO ⁺ C ₄ H ₈ ⁺ + NO C ₄ H ₇ ⁺ + HNO C ₄ H ₇ N ⁺ + (OH) C ₄ H ₆ N ⁺ + (H ₂ O) C ₂ H ₇ N ⁺ + (C ₂ HO) C ₂ H ₆ N ⁺ + (C ₂ H ₂ O) C ₃ H ₇ ⁺ + (HNCO) C ₃ H ₆ ⁺ + (H ₂ NCO) C ₃ H ₅ ⁺ + (H ₂ NCOH)	86 56 55 69 68 45 44 43 42 41	0.32 -0.41 -0.66 -4.73 -0.01 -2.93 -1.97 -0.39 -2.18	1.4 [1.7] 0.73 0.09 0.05 0.02 0.01 0.01 0.03 0.05 0.03	1.1 [1.6] 0.60 0.14 0.08 0.02 0.01 0.02 0.03 0.06 0.03	0.9 [1.6] 0.45 0.17 0.14 0.03 0.01 0.02 0.05 0.06 0.05	0.6 [1.6] 0.25 0.25 0.12 0.02 0.02 0.07 0.07 0.07
avg tot. energy, eV				0.11	0.17	0.27	0.37

^a The collision rate constant, k_c , is given in brackets next to the experimental rate constants. All rate constants are given in units of $10^{-9} \text{ cm}^3 \text{ s}^{-1}$. The average energy in eV for the reaction of NO⁺ with 1-butene is given for the temperatures studied. The reaction enthalpy at 298 K, $\Delta H_{\text{rxn}}^{298}$, is given in eV.

second quadrupole mass spectrometer. The depletion of the reactant ion over a previously measured reaction time is recorded as a function of the butene concentration to get the rate constants. The relative uncertainties in the rate constants are $\pm 15\%$ and the absolute uncertainties are $\pm 25\%$.¹⁹

The product distributions are measured in two steps as described previously.¹⁰ All branching fractions are measured by extrapolating to zero reactant flow. First, the branching fractions are measured at low mass resolution in the second quadrupole mass spectrometer to minimize mass discrimination among the various C_n product ions. Then, the product distributions for a particular C_n peak are measured at high mass resolution to get the branching among the products differing by one mass unit. The overall branching fraction for a single product ion is simply the product of the low and high mass resolution values. A correction is also made for the ¹³C isotopic products.^{14,16} The relative errors in the product branching fractions are $\pm 25\%$.¹⁰

The reactant gases have been used as obtained from the manufacturer (Aldrich). The 1-butene and the isobutene are both 99+% pure. The *cis*-2-butene is comprised of 95% *cis* and 5% *trans*-2-butene, while the *trans*-2-butene is 99+% pure. Consequently, the *trans*-2-butene rate constants are measured first and the *cis*-2-butene rate constants are corrected for the *trans* component of the sample. A single product occurs for both isomers, simplifying the product distribution measurements.

Results and Discussion

Table 1 shows the rate constants and branching fractions for the reactions of NO⁺ with the C₄H₈ isomers from 225 to 500 K. The reactants are listed in order of increasing ionization energy of the isomer. The average total energy available for reaction in eV, $\langle E_{\text{tot}} \rangle$, is also given for the 1-butene reaction. At a given temperature, $\langle E_{\text{tot}} \rangle$, represents the sum of the average collision energy, the average rotational and vibrational energy in the butene molecules (neglecting zero point energy), and any internal energy in the NO⁺ ion, as shown in eq 1.

$$\langle E_{\text{tot}} \rangle = \langle E_{\text{trans}} \rangle + \langle E_{\text{vib}}^{\text{C}_4\text{H}_8} \rangle + \langle E_{\text{rot}}^{\text{C}_4\text{H}_8} \rangle + \langle E_{\text{in}}^{\text{NO}^+} \rangle \quad (1)$$

The average collision energy, $\langle E_{\text{trans}} \rangle$, and the average rotational energy of C₄H₈, $\langle E_{\text{rot}}^{\text{C}_4\text{H}_8} \rangle$, are both $3/2k_B T$. The average internal energy of NO⁺, $\langle E_{\text{in}}^{\text{NO}^+} \rangle$, is principally the average rotational energy given by $k_B T$, because a negligible amount of the NO⁺ ($v'' > 0$) levels are thermally populated over the experimental temperature range. The average vibrational energy in the butene molecule, $\langle E_{\text{vib}}^{\text{C}_4\text{H}_8} \rangle$, represents an ensemble average over a Boltzmann distribution in the harmonic approximation.

The calculated vibrational frequencies of Schei et al.²¹ for the *cis*-2-, *trans*-2-, and isobutene isomers have been used to determine their average vibrational energies. The vibrational frequencies for 1-butene are taken from the fundamental frequencies calculated by Gallinella and Cadioli²² using density functional theory (DFT) and fit to their Fourier transform Infrared (FT-IR) spectrum of 1-butene vapor measured at 298 K to assign the fundamentals for the *syn* and *skew* isomers. The terminal methyl group eclipses the α -CH₂ in the *syn* isomer, whereas the methyl group is staggered by around 120° in the *skew* isomer. The enthalpy difference between the two isomers measured by Gallinella and Cadioli²² shows that the *syn* form is slightly more stable, but only by about 1 kJ mol⁻¹. The frequencies previously calculated by Schei et al. for 1-butene using valence force fields (VFF) agree with the more recently calculated frequencies²² to within 5% for both 1-butene isomers. Ab initio vibrational frequencies calculated by Baer and co-workers²³ are in similar agreement with the latest *skew* frequencies. Overall, the average vibrational energies calculated using the three sets of frequencies differ by $\leq 5\%$.

The average total energy shown in Table 1 reflects the average vibrational energy for the *skew* isomer of 1-C₄H₈ using the most recently calculated frequencies,²² which provides a lower bound for this number. The energies of the other butene isomers differ from 1-C₄H₈ by $< 8\%$ at the highest temperatures and are not shown. A detailed discussion of the results is given in the following sections for each isomer.

A. *cis*- and *trans*-2-Butene. Both isomers of 2-butene react

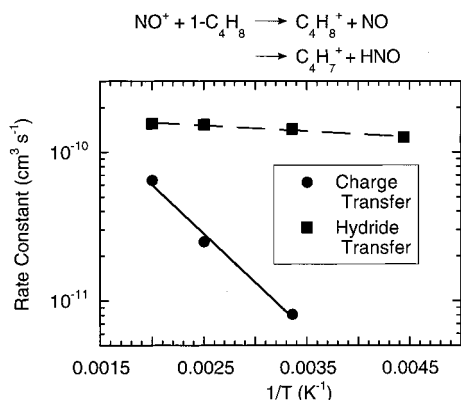


Figure 1. Rate constants in $\text{cm}^3 \text{s}^{-1}$ for the charge transfer and hydride transfer reaction channels as a function of inverse temperature. The lines represent a fit to the Arrhenius equation given as $k = A \cdot \exp(-E_a/RT)$ using the parameters in Table 2.

with NO^+ at the Su–Chesnavich collision rate^{24,25} at all temperatures. The reactions proceed almost exclusively via nondissociative charge transfer, and both reactions are exothermic by 0.15 eV. These large rate constants are typical for near resonant charge-transfer processes at thermal collision energies.^{20,26} The branching fraction at 225 K is given as >99%, because a small amount of an association product is observed. However, this product comprises less than 1% of the total product signal.

B. Isobutene. The reaction of isobutene with NO^+ also proceeds at the Su–Chesnavich collision rate^{24,25} at all temperatures. Bowers and co-workers¹⁸ have obtained a rate constant for this reaction of $1.27 \times 10^{-9} \text{ cm}^3 \text{ s}^{-1}$ in an FT-ICR that is about 25% lower than the present value. This difference is well within the combined experimental errors. Charge transfer is the only product observed in the ICR experiment, and it is the predominant channel in the VT-SIFT. However, a significant fraction of an association product is observed in the flow tube experiment at temperatures of 400 K and below. The association channel displays a negative temperature dependence, as expected. Charge transfer is only 0.02 eV exothermic. Therefore, collisions with the ca. 0.5 Torr of He buffer in the flow tube can remove enough energy from any association complex that forms during charge exchange, thus stabilizing it. The FT-ICR experiments have been conducted at pressures more than 2 orders of magnitude lower than the flow tube measurements,¹⁸ resulting in a significant reduction in the probability for collisional stabilization of the association complex.

C. 1-Butene. In contrast to the other reactions, numerous products are formed. The rate constants are smaller than the Su–Chesnavich collision rate constants^{24,25} and decrease as the temperature increases. The negative temperature dependence is consistent with a reaction involving complex formation, as evidenced by the predominance of the association channel at most temperatures. Numerous other products are also observed, as seen in Table 1. Hydride transfer is the next most abundant product after association. This channel increases with increasing temperature. Charge transfer, which is endothermic, also increases with temperature. The individual rate constants for the charge transfer and hydride transfer channels are shown in Figure 1 in Arrhenius form. Activation energies have been extracted from the fitting parameters and are listed in Table 2. Charge transfer is 0.32 eV endothermic, which is larger than the fitted activation energy of only 0.15 eV. The preexponential factor for this channel is almost exactly equal to the collision rate.

TABLE 2: Fitting Parameters for the Reaction of NO^+ with 1-butene (C_4H_8) Using the Expression $k = A \cdot \exp(-E_a/RT)$

	A ($\text{cm}^3 \text{s}^{-1}$)	E_a (eV)
$\text{NO}^+ + 1\text{-C}_4\text{H}_8 \rightarrow \text{C}_4\text{H}_8^+ + \text{NO}$	1.22×10^{-9}	0.15
$\text{NO}^+ + 1\text{-C}_4\text{H}_8 \rightarrow \text{C}_4\text{H}_7^+ + \text{HNO}$	1.89×10^{-10}	0.01

It is also informative to look at how the reactivity changes as a function of total energy. The average reaction energy available increases substantially at higher temperatures due in large part to butene vibrations. At 500 K, the average energy exceeds the charge transfer endothermicity. An Arrhenius type plot of rate constant vs 1/total energy (not shown) yields an activation energy of 0.72 eV, considerably higher than the endothermicity. The fact that the charge transfer rate constant at 500 K is only 3.6% of the collision rate and that the average total energy is greater than the endothermicity indicates that all forms of energy are not efficient in overcoming the endothermicity. The total rate constant is only 38% of the collision rate, so competition with another channel cannot account for this. The high-energy tail arising from the spread in the thermal energy distributions at 298–400 K most likely accounts for the small amount of C_4H_8^+ observed at low temperature.

Hydride transfer from C_4H_8 to NO^+ yielding C_4H_7^+ and HNO is 0.41 eV exothermic for loss of a secondary alkyl hydrogen, which is the lowest energy C–H bond for 1-butene.²⁷ The reaction proceeds with an activation energy of 0.01 eV, indicating a barrier to reaction, consistent with the small positive temperature dependence in Figure 1. Hydride transfer is often an inefficient process.^{20,28}

The energetically accessible channels for the remaining products require significant atomic rearrangement and chemical bond formation,^{29,30} perhaps through insertion mechanisms occurring in the complex. Forming these structures is sterically unfavorable and requires substantial rearrangement, which shows up in the small rate constants that increase with temperature for these channels. The total fraction of these channels increases to as much as 37% at 500 K. The positive temperature dependence of these small rate coefficients also implies that potential barriers exist.

The most stable structures for several of the minor products contain an N–C–O linkage.^{29–31} Ab initio studies on the structures of the neutral molecules CH_3NO ,³² CH_2NO ,³¹ and CHNO ^{33–35} all show that the most energetically stable isomers contain NCO bonds. Several transition state structures available through different pathways lead to the lowest energy neutral species,³¹ so these species may be readily produced from various access points along the potential energy surfaces. Similar rearrangements probably occur in the analogous ionic species for NO incorporation. The NO^+ ion would most likely be attracted to the double bond of 1-butene. Approaching this end would facilitate analogous rearrangements observed with the neutral molecules to form the more stable NCO species.^{31,34,35} Spanel and Smith have observed similar ionic products, in which the NO is incorporated in the reaction of NO^+ with 1-pentene in a SIFT at 298 K.¹³

To test for N inclusion in the ionic products, $^{15}\text{NO}^+$ produced in the source from the natural abundance in NO is selectively injected into the flow tube. This isotopically labeled experiment indicates that N is incorporated in the unlabeled product at $m/z = 69$. The ion could have the formula $\text{C}_3\text{H}_3\text{NO}^+$; however, a $\text{C}_4\text{H}_7\text{N}^+$ pyrrole structure must be assumed for this product ion for the reaction to be exothermic.^{29,30,36} Similar experiments are not feasible for verifying that the products at $m/z = 44, 45$, and 68 contain N, because of the spectral congestion and the small signal levels. Amine structures are nevertheless energetically

possible for these products.^{29,30} For consistency, the amine products are listed in Table 1 for those three product ions; however, the energetically accessible products may alternatively contain both N and O. The most stable structures would have NCO bonds in the fragments.^{29,30}

Some other possible sources of these small product channels can be discounted. One potential problem can be break-up upon sampling at the nose cone aperture. Sampling voltages of 2–5 V are typically used to maximize signal-to-noise ratio and minimize perturbations. However, the branching fractions measured are independent of the sampling voltage from 3.5 to 7 V, exceeding the normal operating range. As previously mentioned, N₂ is added to quench NO⁺, producing a small amount of N₂⁺ in the flow tube. N₂⁺ reacts with 1-butene in the VT-SIFT via dissociative charge transfer to give several products of the same mass as the reaction with NO⁺. However, the N₂⁺ ions represent <2% of the reactant ions present in the flow tube, so the major products of the N₂⁺ reaction would contribute <1% of any individual product signal observed. Alternatively, an insufficient flow of N₂ upstream of the reaction region may not completely quench NO⁺ ($X, v'' > 0$). Normally, it is easy to calculate this contribution, but the experimental quenching rates vary by an order of magnitude.^{37–39} The branching fractions at 298 K have therefore been measured as a function of N₂ flow to check for a potential interference from vibrationally excited NO⁺. The only significant difference is that a small C₄H₈⁺ signal arises at lower N₂ flows. Little of this ion is seen at larger flows, implying that vibrationally excited NO⁺ results in more of the endothermic charge-transfer C₄H₈⁺ being produced. It is subsequently possible that a small amount of vibrationally excited NO⁺ may cause a small part of the charge-transfer signal observed below 500 K.

Rapid secondary reactions of the primary product ions such as C₃H₅⁺ and C₄H₇⁺ with residual 1-butene can also give the products observed in the primary reaction.^{40–42} The contributions from these additional reactions would not extrapolate to zero at zero reactant flow if the secondary chemistry is much faster than the primary chemistry. In this case, the primary reaction with NO⁺ is relatively fast compared to the secondary reactions,²⁰ ruling out this potential artifact.

Conclusions

Rate constants and branching fractions for the reactions of NO⁺ with the isomers of butene have been measured from 225 to 500 K. The 1-butene reaction is quite complex, producing 10 different products. Association is the most abundant channel over the 225–500 K temperature range. When charge transfer is not energetically accessible, complex formation controls the reactivity. However, charge transfer becomes the driving reaction as temperature increases, with a rate constant that increases rapidly at higher temperatures. This increase coincides with a concomitant decrease in the association rate constant. Hydride transfer from 1-butene also makes a significant contribution, but the rate constant has a much weaker temperature dependence. Most of the other channels have branching fractions below 0.07 and individually make minor contributions to the total reactivity. However, the sum of the minor channels is substantial. The reaction of NO⁺ with 1-butene approaches the collision rate, but the rate constants show a negative temperature dependence, because the major channel is association. The hydrocarbon ions C₄H₇⁺ from hydride transfer and C₄H₈⁺ from charge transfer are also observed, accompanied by several other products arising from rearrangement involving the formation of new chemical bonds. The reactions of the remaining butene

isomers proceed at the collision rate mainly by charge transfer. However, a significant association channel also occurs in the isobutene reaction, where the charge transfer reaction is only slightly exothermic.

Acknowledgment. A.A.V. gratefully acknowledges Hal Johnston as a wonderful mentor for introduction to both research and atmospheric chemistry. The authors would like to thank Susan Arnold for helpful discussions. We would also like to thank John Williamson and Paul Mundis for technical support. This research has been supported by the Air Force Office of Scientific Research under Project No. 2303EP4. A.J.M. is an Air Force Research Laboratory Scholar.

References and Notes

- (1) Calcote, H. F. *Combust. Flame* **1981**, *42*, 215.
- (2) Olson, D. B.; Calcote, H. F. Ionic Mechanism of Soot Formation in Premixed Flames. In *Particulate Carbon Formation During Combustion*; Sieglia, D. C., Smith, G. W., Eds.; Plenum: New York, 1981; p 177.
- (3) Olson, D. B.; Calcote, H. F. "Ions in Fuel-Rich and Sooting Acetylene and Benzene Flames"; Eighth International Symposium on Combustion, 1981.
- (4) Henderson, R. E. AGARD Report R-824, NATO, 1997.
- (5) Nagashima, T.; Kitamaru, H.; Obata, S. In *Proceedings of the XIII International Symposium on Air Breathing Engines (ISABE)*; Chattanooga, TN, 1997; p 366.
- (6) Mathur, T.; Streby, G.; Gruber, M.; Jackson, K.; Donbar, J.; Donaldson, W.; Jackson, T.; Smith, C.; Billig, F. "Supersonic Combustion Experiments with a Cavity-Based Fuel Injector"; AIAA 99–2102, 35th AIAA/ASME/SAE/ASEE Joint Propulsion Conference and Exhibit, 1999, Los Angeles, CA.
- (7) Gruber, M. R.; Baurle, R. A.; Mathur, T.; Hsu, K.-Y. "Fundamental Studies of Cavity-Based Flameholder Concepts for Supersonic Combustors"; AIAA 99–2248, 35th AIAA/ASME/SAE/ASEE Joint Propulsion Conference and Exhibit, 1999, Los Angeles, CA.
- (8) Calcote, H. F.; Gill, R. J. *Comparison of the Ionic Mechanism of Soot Formation with a Free Radical Mechanism*; Bockhorn, H., Ed.; Springer-Verlag: Heidelberg, **1994**; p 471.
- (9) Spanel, P.; Smith, D. *J. Chem. Phys.* **1996**, *104*, 1893.
- (10) Arnold, S. T.; Viggiano, A. A.; Morris, R. A. *J. Phys. Chem. A* **1997**, *101*, 9351.
- (11) Arnold, S. T.; Viggiano, A. A.; Morris, R. A. *J. Phys. Chem. A* **1998**, *102*, 8881.
- (12) Arnold, S. T.; Morris, R. A.; Viggiano, A. A. *J. Phys. Chem. A* **1998**, *102*, 1345.
- (13) Spanel, P.; Smith, D. *Int. J. Mass Spectrom.* **1998**, *181*, 1.
- (14) Arnold, S. T.; Williams, S.; Dotan, I.; Midey, A. J.; Morris, R. A.; Viggiano, A. A. *J. Phys. Chem. A* **1999**, *103*, 8421.
- (15) Arnold, S. T.; Dotan, I.; Williams, S.; Viggiano, A. A.; Morris, R. A. *J. Phys. Chem. A* **2000**, *104*, 928.
- (16) Midey, A. J.; Williams, S.; Arnold, S. T.; Dotan, I.; Morris, R. A.; Viggiano, A. A. *Int. J. Mass Spectrom.* **2000**, *195*, 327.
- (17) Williams, S.; Midey, A. J.; Arnold, S. T.; Morris, R. A.; Viggiano, A. A.; Chiu, Y.-H.; Levandier, D. J.; Dressler, R. A.; Berman, M. R. *J. Phys. Chem. A* **2000**, in press.
- (18) Beggs, C. G.; Kuo, C.-H.; Wyttenbach, T.; Kemper, P. R.; Bowers, M. T. *Int. J. Mass Spectrom. Ion Proc.* **1990**, *100*, 397.
- (19) Viggiano, A. A.; Morris, R. A.; Dale, F.; Paulson, J. F.; Giles, K.; Smith, D.; Su, T. *J. Chem. Phys.* **1990**, *93*, 1149.
- (20) Ikezoe, Y.; Matsuoka, S.; Takebe, M.; Viggiano, A. A. *Gas-Phase Ion-Molecule Reaction Rate Constants Through 1986*; Maruzen Co., Ltd.: Tokyo, 1987.
- (21) Schei, S. H. *Acta Chem. Scand. A* **1984**, *38*, 377.
- (22) Gallinella, E.; Cadioli, B. *Vibr. Spectrosc.* **1997**, *13*, 163.
- (23) Booze, J. A.; Schweinsberg, M.; Baer, T. *J. Chem. Phys.* **1993**, *99*, 4441.
- (24) Su, T.; Chesnavich, W. J. *J. Chem. Phys.* **1982**, *76*, 5183.
- (25) Su, T. *J. Chem. Phys.* **1988**, *89*, 5355.
- (26) Dressler, R. A.; Levandier, D. J.; Williams, S.; Murad, E. *Comments At. Mol. Phys.* **1998**, *34*, 43.
- (27) Bauschlicher, C. W. *Chem. Phys. Lett.* **1995**, *239*, 252.
- (28) Meot-Ner, M.; Field, F. H. *J. Am. Chem. Soc.* **1975**, *97*, 2014.
- (29) Lias, S. G.; Bartmess, J. E.; Liebman, J. F.; Holmes, J. L.; Levin, R. D.; Mallard, W. G. *J. Phys. Chem. Ref. Data* **1988**, *17*, Supplement 1, 1.
- (30) Lias, S. G.; Bartmess, J. E.; Liebman, J. F.; Holmes, J. L.; Levin, R. D.; Mallard, W. G. Ion Energetics Data. In *NIST Chemistry WebBook, NIST Standard Reference Database Number 69*; Mallard, W. G., Linstrom, P. J., Eds.; NIST: Gaithersburg, 1998; pp (http://webbook.nist.gov).

- (31) Shapley, W. A.; Backsay, G. B. *J. Phys. Chem. A* **1999**, *103*, 4505.
(32) Jensen, J. O.; Krishnan, P. N.; Burke, L. A. *J. Mol. Struct. (THEOCHEM)* **1996**, *370*, 245.
(33) Pinnavaia, N.; Bramley, M. J.; Su, M. D.; Green, W. H.; Handy, N. C. *Mol. Phys.* **1993**, *78*, 319.
(34) Mebel, A. M.; Luna, A.; Lin, M. C.; Morokuma, K. *J. Chem. Phys.* **1996**, *105*, 6439.
(35) Shapley, W. A.; Backsay, G. B. *J. Phys. Chem. A* **1999**, *103*, 6624.
(36) Chong, D. P.; Hu, C. H. *J. Chem. Phys.* **1998**, *108*, 8950.
(37) Ferguson, E. E. *J. Phys. Chem.* **1986**, *90*, 731.
(38) Morris, R. A.; Viggiano, A. A.; Dale, F.; Paulson, J. F. *J. Chem. Phys.* **1988**, *88*, 4772.
(39) Wyttenbach, T.; Bowers, M. T. *J. Phys. Chem.* **1993**, *97*, 9573.
(40) Abramson, F. P.; Futrell, J. H. *J. Phys. Chem.* **1968**, *72*, 1994.
(41) Munson, M. S. B. *J. Am. Chem. Soc.* **1968**, *90*, 83.
(42) Sieck, L. W.; Lias, S. G.; Hellner, L.; Ausloos, P. *J. Res. Nat. Bur. Stand.* **1972**, *76A*, 115.